



Iterative local remeshing for locally-injective deformations

Master Thesis

Antoine Demont

University of Fribourg

May 2024



Abstract

To run simulations or model three-dimensional objects, we need a way to represent them. This is achieved using a mesh, whose vertices collectively form the shape of the object. When subjected to deformations, meshes can develop degenerate or inverted elements. To address this issue, we perform remeshing on the represented object, which can be done either globally or locally. Global remeshing generates a new mesh that is best suited to the deformed object, whereas local remeshing focuses on identifying and improving the critical elements near the problem areas. In this work, we present an implementation of a local remeshing algorithm for locally-injective deformations, in which each remeshing operation can be reverted. This allows us to restore the mesh to its initial state and topology after any deformation. The remeshing process involves identifying the problematic elements and addressing each through four iterative passes: *topological*, *contraction*, *insertion*, and *smoothing* pass. Each pass aims to enhance the mesh quality through multiple techniques such as edge and face removal, edge contraction, vertex insertion, or smoothing.

Prof. Dr. David Bommes, Computer Graphics Group, University of Bern, Supervisor Valentin Nigolian, Computer Graphics Group, University of Bern, Assistant

Contents

1	Introduction	4
2	Related work	5
2.1	World space and material space	6
2.2	Types of Meshes	6
2.3	Hill climbing algorithms	7
3	Mesh deformations	8
3.1	Mesh evaluation	8
3.1.1	Triangular meshes	8
3.1.2	Tetrahedral meshes	9
3.1.2.1	Computing the Jacobian	9
3.2	Bad elements	10
4	Remeshing	12
4.1	General remeshing algorithm	12
4.2	Control mesh	13
4.3	Triangular meshes	13
4.3.1	Topological pass	13
4.3.2	Insertion pass	14
4.3.3	Smoothing pass	15
4.4	Tetrahedral meshes	16
4.4.1	Topological pass	16
4.4.2	Insertion pass	18
4.4.2.1	Chebyshev Center	19
4.4.2.2	Insertion algorithm	19
4.4.3	Smoothing pass	21
4.5	Complete algorithm	22
5	Results	24
5.1	Triangular meshes	24
5.1.1	Stretch	25
5.1.2	Compress	25
5.1.3	Finding the right threshold	26
5.2	Tetrahedral meshes	27
5.2.1	Performance of passes	27
5.2.2	Twist	28
5.2.2.1	Influence of the Energy Threshold	29
5.2.2.2	Influence of the Timestep Size	30
5.2.2.3	Handling greater deformations	32

<i>CONTENTS</i>	3
5.2.3 Stretch	32
5.2.3.1 Influence of the Energy Threshold	33
5.2.3.2 Influence of the Timestep Size	34
5.2.3.3 Handling bigger deformations	36
5.2.4 Impact of the control mesh	37
5.2.5 Reverse deformation	37
6 Conclusion	38
6.1 Weaknesses and future work	38
6.2 Use of AI tools	39

1

Introduction

At first, the process of making cartoons consisted of drawing successive pictures and sequencing them to create the illusion of movement. Immobile elements could be reused between frames, but any element in motion had to be redrawn for every movement. Once computer-generated images and 3D modeling came forth, following this method would be naive and time-inefficient. In an animated movie, it would be prohibitively expensive for an animator to remodel a character each time the character moves a finger or opens their mouth to speak. Fortunately, unlike static drawings, three-dimensional objects can be altered by manipulating their geometry. This introduces the concept of *mesh deformation*, where we alter the shape of a 3D object by moving the vertices that compose it.

Say we want to perform a physical simulation of an iron bar bending. To represent it, we use a tetrahedral mesh, which will hold data about both the surface and the inside of the object. As the bar bends, the vertex distribution will stray from its initial representation. This could cause some of them to create tetrahedra of bad quality or inverted elements. If we were to use the mesh to compute physical properties, having such irregularities could not translate from the simulation to the real world and would inevitably produce incorrect results. So, we observe that the space of possible deformations is constrained by the mesh used. To mitigate it, we need to operate on the mesh with the intent of matching more closely to the new shape of the object. This operation is called *remeshing*. In this project, we will present an implementation of a local remeshing algorithm for locally-injective deformations. Meaning it is responsible to, in a first step, identify the conflicting elements of the mesh, then operate on the mesh to either remove them or increase their quality to an acceptable level for each one successively. Lastly, any remeshing operations or deformations on the mesh can be reverted to a previous state.

In Chapter 2, we will first introduce the process to ensure bijection on the operations as well as the types of mesh used in the project. We will explain the concept of hill climbing algorithms and then, in Chapter 3, present how to grade mesh quality during deformation. In Chapter 4 we go into more detail about the implementation of the algorithm in both two and three dimensions. Finally, in Chapter 5, we evaluate its performances on meshes subjects to varying deformations along with discussing the optimal setting of parameters.

2

Related work

In this chapter, we will briefly present the paper we based this project on, as well as discuss the work related to it. This contains the topic of remeshing, the introduction of a different space mapping for meshes, the two types of mesh used for object representation and the concept of hill climbing methods.

This project is based on the work of Wicke et al. [12], who describe the implementation of a dynamic local remeshing algorithm and its use in physics-based simulations of elastoplastic materials.

Remeshing is a wide field, nonetheless, we can identify two main approaches to the problem: global or local remeshing. The first consist of remeshing the entire domain when critical conditions are met. This approach is used in the work of Bargeuil et al. [3] as well as Wojtan and Turk [13]. A disadvantage to this way of tackling remeshing is, that regardless of the quality of the "good" elements, the complete mesh must be rebuilt from the ground up every time it is performed, inducing inefficient operations. This inefficiency is particularly evident when only a local area of the mesh is in poor condition while the rest remains in good or acceptable shape. Wicke et al. [12] also state that global remeshing accumulates large numerical errors in simulations, called *artificial diffusion*, due to the need to resample physical properties from an old to a new mesh. By changing completely the mesh at each remeshing step, the diffusion of physical properties, for example, the transmission of forces, can differ from a natural path due to the changes in the mesh topology. [12] show in their simulations that some element of the strain field exaggerated plastic-like behavior of purely elastic objects due to the *artificial diffusion*.

In the second approach, local remeshing, we aim to identify and replace only the low-quality elements from the mesh. By minimizing the changes on the mesh, we reduce the *artificial diffusion* mentioned before. Since most of the mesh is left untouched, its topology is similar for each deformation step, and thus the transmission of physical properties flows through more constantly. Being a sum, having as few changes as possible keeps the *artificial diffusion* to the lowest. Additionally, with local remeshing, coarsening the mesh where it is unnecessarily detailed or inversely adding details in smaller parts of the mesh is automatically done as these regions are more likely to create bad elements. Thus creating a better match between the shape of the object and the mesh.

2.1 World space and material space

To ensure the bijection of all operations, we copy the mesh into a world space representation and a material space representation (fig. 2.1). All the deformations of the simulation will be applied in world space whereas the material space will remain unchanged. Each remeshing operation is applied to both spaces and has to be valid for each of them. This bijective state guarantees that any operation can be reverted. Making it possible to reset the world space mesh to its initial state or rest state, simulate elasticity, or any other temporary deformation. In this regard, this project deviates from the original implementation by Wicke et al. [12]. The goal of their program was to conduct elastoplastic simulations. An elastic material will retrieve its original shape after being subjected to a deformation. Being able to revert operations is a good tool to simulate elasticity. By doing so, we can navigate between a stretched shape of an object and its rest state by reverting the stretching applied to it. We extended this relation between world space and material space to other deformations. Rather than simulating physical properties, we split the deformation into successive predetermined positions and performed the remeshing based on them. With this, we can extend this method to continuous deformations, where we go through successive positions to reach a final shape. Here, being able to revert operations allows one to navigate freely between the deformation steps performed.

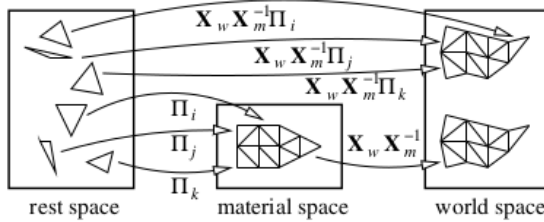


Figure 2.1: Relation between material and world space, taken from [12]. Deformations occur in the world space. Remeshing is performed in both material and world space, allowing to revert deformations to a previous rest space.

2.2 Types of Meshes

Wicke et al.[12] is using a tetrahedral mesh for the representation of 3-dimensional objects. In this work, we will adapt their algorithm to both 2-dimensional and 3-dimensional meshes.

For the 2-dimensional representation, we work on a flat triangular mesh composed of a plane tessellated with triangles. For 3D meshes, the triangles used in 2D are replaced by tetrahedra. A visual comparison of the two mesh types is shown in figure 2.2. Using a triangle mesh was a stepping stone into the program's implementation, hence the use of a simpler planar setting. With more attention to two-dimensional remeshing, one could extend the 2D implementation to also work with three-dimensional objects similar to our tetrahedral remeshing algorithm. The difference in dimensions would mean for simulations that an object represented using a triangular mesh would only be composed of its surface, making it completely hollow, whereas one using a tetrahedral mesh is filled. Since a 2-dimensional mesh does not have to care about the inside of the object, it is a more lightweight and simple means of representing it. For more accurate results, using a 3-dimensional mesh is recommended as it can model different properties between the surface and the inside of the object as well as the transfer of forces through it.

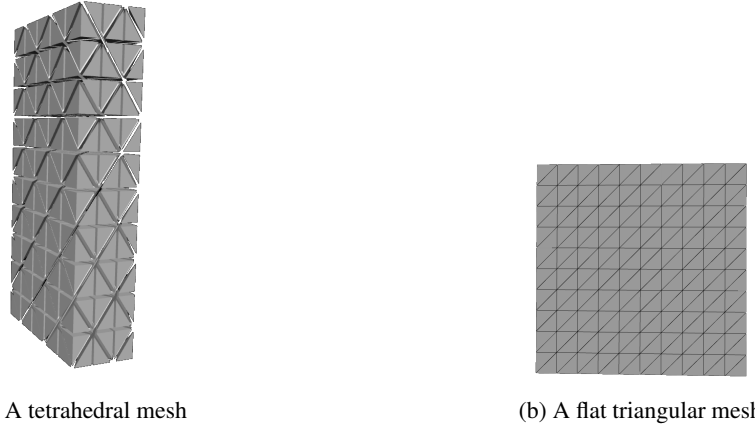


Figure 2.2: The two types of meshes used in this project. Representing higher-dimension objects (volumes) requires using higher-dimension primitives (tetrahedra versus triangles)”

2.3 Hill climbing algorithms

The original paper uses a hill climbing method. It involves starting from a current state and iteratively attempting to achieve the optimal state by consistently taking actions that bring us closer to it. For example, to find the top of a hill we start from its foot and only take the steps allowing us to reach a higher altitude until all the steps we can take lead us downwards, meaning we have reached the summit. This is a simple way of finding an optimum but suffers from one clear flaw: local optima. When taking the curve in figure 2.3 we see that the clear maximum is situated at point *C*. But if our only knowledge is the gain we get from our next step, then, starting from *A*, the first step we take determines whether our efforts are in vain or lead us to the global maximum. By going in the negative direction of the *x*-axis we will inevitably reach the peak *B* and falsely set it as the maximum. This issue can be mitigated by performing multiple attempts. To go back to the literal interpretation, we take 100 hikers with us who will help us reach the highest hill in the region. But if only one hiker reaches the actual maximum, this means that 99 of them did all their work for nothing. This overhead is something to be tuned to match the need between accuracy and performance.

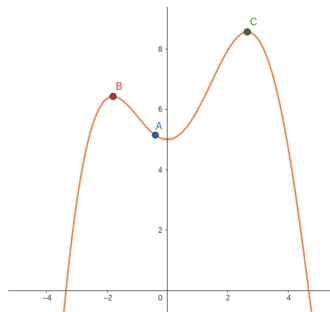


Figure 2.3: Function with a local (*B*) and global (*C*) maximum. During remeshing, with mesh quality *A*, we can improve it by performing an operation o_1 leading us to *B*, a local maximum, or an operation o_2 leading us to *C*, the actual maximum. Without knowledge of the future state of the mesh, both operations are treated as the best solution.

3

Mesh deformations

This chapter presents the different metrics used for evaluating the quality of a mesh and its elements, both in two and three dimensions. It also illustrates the occurrence of bad elements in a mesh as well as a first insight into how to treat them.

3.1 Mesh evaluation

For our mesh, we want to have all its elements as close as possible to a reference shape. An element too different from it is considered to be bad. To quantify the distance between them we use the following methods: For triangular meshes, we adapt the formula from Wicke et al.[12] to two dimensions. For tetrahedral meshes, we introduce another metric for quality: the *symmetric dirichlet energy*.

3.1.1 Triangular meshes

In [12], the quality of a tetrahedron is equal to:

$$6\sqrt{2}V \frac{\ell_{harm}}{\ell_{rms}^4} \quad (3.1)$$

with V the volume, ℓ_{harm} the *harmonic mean* of the tetrahedron's edge lengths and ℓ_{rms} the *root-mean-squared* edge length. [12] say this measure is bounded in $[0, 1]$, we can assume that negative volumes are treated as having a quality of 0. A quality of 1 is attributed to an equilateral tetrahedron and 0 to a degenerate one, where all the vertices are coplanar.

We find a similar approach for triangles in [5] by Freitag. The difference of an element with a reference equilateral triangle of side length 1 is measured by:

$$4\sqrt{3}A \frac{1}{\sum_{i=1}^3 l_i^2} \quad (3.2)$$

with, similar to eq. 3.1, A the area and l_i the i th edge of the triangle. Equivalent to eq. 3.1, a quality of 1 means an equilateral triangle and 0 for a degenerate triangle. To detect inverted triangles, we compute the signed area of the triangle such that any value of $A < 0$ indicates an inverted triangle.

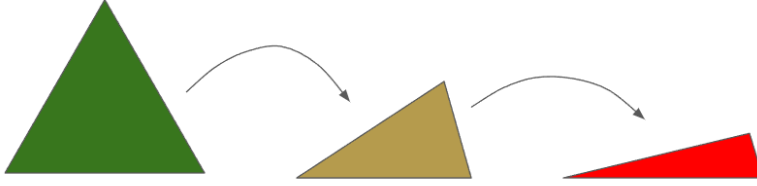


Figure 3.1: Triangle losing quality. As we deform it, the difference with the reference (in green) increases, resulting in a lower *quality*.

3.1.2 Tetrahedral meshes

$$E_{dirichlet}(t) = \|\mathcal{J}_t\|_2 + \|\mathcal{J}_t^{-1}\|_2 - 6, \begin{cases} \text{if } \det(\mathcal{J}) > 0, \\ \text{otherwise, } \infty \end{cases} \quad (3.3)$$

with $\|\cdot\|_2$ the Frobenius norm and \mathcal{J}_t the *jacobian matrix* of the mapping between a tetrahedron t and the reference scaled by a coefficient of the volume, to reduce the penalty on smaller regular tetrahedra. The detailed computation of the jacobian is presented in sec. 3.1.2.1. Note that the reference tetrahedron can be adapted. For example, one could set the reference tetrahedron's value to the best of the mesh before any deformation is applied, thus measuring more closely the distortion between the current and the initial state of the mesh. With this method, a perfect element, meaning an element that has no stretching with respect to the reference, has an energy of 0. For any other element, we invert the positive value given by the *symmetric dirichlet energy*. With this, the bigger the energy, the worse the quality of the element will be.

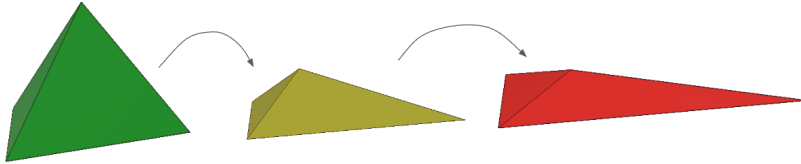


Figure 3.2: Tetrahedron gaining energy. As we deform it, the difference with the reference (in green) increases, resulting in a higher *dirichlet energy*.

3.1.2.1 Computing the Jacobian

To compute the Jacobian \mathcal{J}_t of tetrahedron t , we refer to the work of [6]. Given a map \vec{u} , we take \vec{a}_i the vectors forming the columns of the Jacobian matrix \mathcal{J} . We then set the dual basis $\vec{b}_k = \vec{a}_i \times \vec{a}_j$, such that i, j, k are a cyclic permutation of the 3 columns indices from \mathcal{J} . With it we obtain $\mathcal{J}^T \mathcal{J} = \sum_i |\vec{a}_i|^2$ and $\frac{\delta \det(\mathcal{J})}{\delta \vec{a}_i} = \vec{b}_i$.

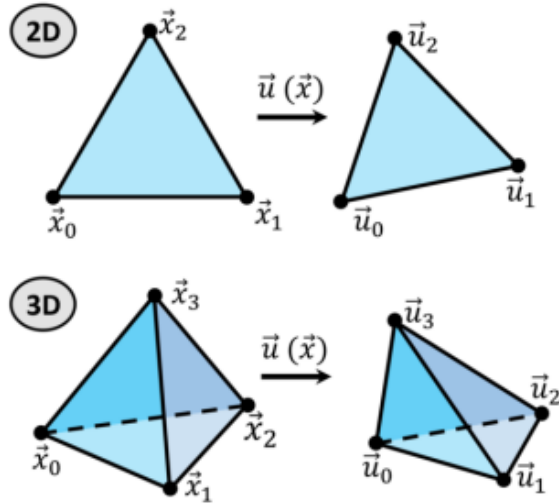
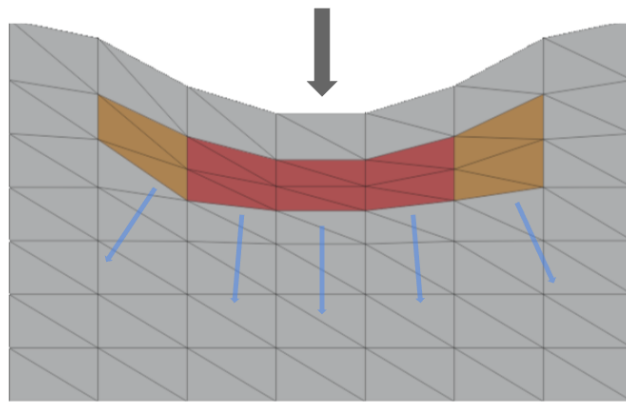


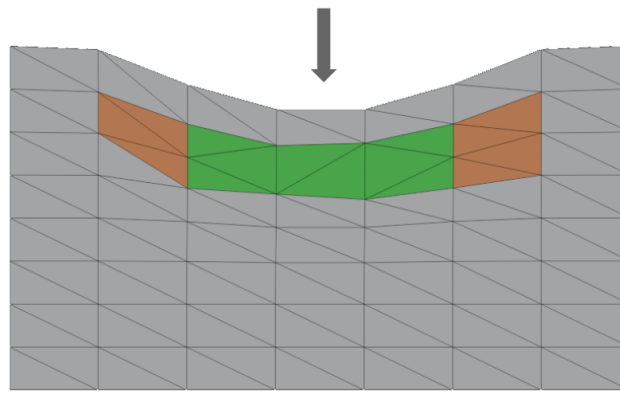
Figure 3.3: Taken from [6], "On each simplex the map $\vec{u}(\vec{x})$ is affine and is entirely defined by the position of the vertices of the domain simplex $\{\vec{x}_i\}$ and its image $\{\vec{u}_i\}$."

3.2 Bad elements

Now that we can identify bad elements in a mesh, we will discuss when and how those can appear. In figure 3.4a, we see that as we apply a force to the mesh, some of the vertices are getting closer to each other. Continuing this deformation without any remeshing and restriction will inevitably lead to some inversions in the geometry, producing visual artifacts during render or inaccurate simulations. Since we move elements of the mesh without constraints, the vertices of some elements can move past their neighbors, first creating degenerate elements and then inverted ones. By performing remeshing operations, we aim to keep the shape of the object but change the topology of the bad elements to stay within acceptable quality values. Another option would be to limit the vertices' movements to avoid creating low-quality elements but this approach would mean that some deformations could not be applied to the object. Since some would inevitably create low-quality elements on the mesh.



(a) Mesh with bad elements. An external force (in gray) is applied to the mesh, compressing the top boundary and its neighboring triangles.



(b) Same mesh after local remeshing on the red elements.

Figure 3.4: Removal of low-quality elements induced by a force applied to the top boundary of the mesh (gray arrow). Elements of lower quality are highlighted in red and orange.

4

Remeshing

Chapter 4 covers the remeshing algorithm as well as its implementation in two and three dimensions.

4.1 General remeshing algorithm

The overall operation of the algorithm, presented in alg.1, goes as such: We begin by assessing the mesh quality using formulas from Chapter 3 to analyze each element. If an element's quality falls below an empirically set remeshing threshold q_{min} , we add it to a list of candidates for remeshing. After identifying all critical elements, we iteratively improve each one. The remeshing is composed of three sub-parts, in order the *Topological*, *Contraction*, *Insertion* and *Smoothing* passes. As they are complex operations that need an introduction, we will first present each of them before discussing the complete algorithm (alg. 9). After each mesh operation, we evaluate the quality of the new or altered elements. Based on it, we can decide whether to accept or revert the operation in case the quality of the resulting mesh is lower than of the one before.

Algorithm 1 Loop: The overall remeshing algorithm

Require: M a mesh to improve

```
 $B \leftarrow \{\}$ 
for all  $t \in M$  do ▷ Find bad elements
     $q \leftarrow ComputeQuality(t)$ 
    if  $q < q_{min}$  then
         $B \leftarrow B \cup t$ 
    end if
end for
while  $B$  !empty do ▷ Improve mesh
     $e \leftarrow$  Worst element of  $B$ 
     $ImproveElement(e)$ 
end while
```

4.2 Control mesh

As presented in chapter 2, we represent the object in two distinct spaces called world and material space. All deformations occur on the world space representation whereas, in material space, only the topological changes are applied. This method ensures bijection on all mesh operations. When we perform a remeshing step on the world mesh, the operation needs to be validated on the control mesh in the material space. As illustrated in fig. 4.1, after an operation is performed we iteratively check whether it creates a bad element anywhere in the control mesh. In this case, we reset the material space mesh to its previous valid state or update the control mesh if all elements are of sufficient quality. With this, we ensure that any operation is valid in both spaces and that each modification made on the mesh can be reverted to a previous state.

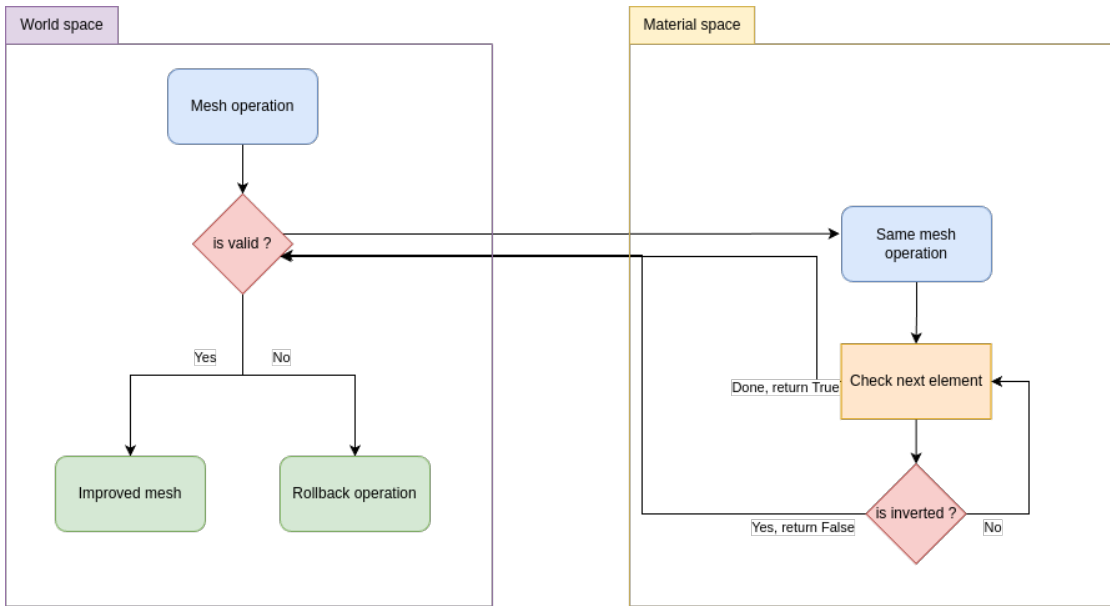


Figure 4.1: Flow diagram for control mesh validation. Each operation in world space has to be validated for every element in the material space before being applied to the mesh.

4.3 Triangular meshes

This section describes the implementation of the topological, insertion and smoothing passes with two-dimensional meshes.

4.3.1 Topological pass

In three-dimensional meshes, Wicke et al.[12] use this pass to remove edges and faces of bad quality. We adapted it to two-dimensional meshes while keeping this idea of low-quality element removal. All without being redundant with the contraction pass presented in alg. 9. To do so we used the edge flip. Shown in fig. 4.2, we see that by flipping an edge both of the bad-quality faces disappear to leave only elements of acceptable quality. With a similar mesh operation as in [12], the algorithm (alg. 2) for the *topological pass* goes as follows: We take the edges of A , the list holding the elements whose quality we want to improve. For each of them, a flip is performed and we check whether the quality of the neighboring triangle improves. Note that boundary edges cannot be flipped as it would modify the shape of the object rather

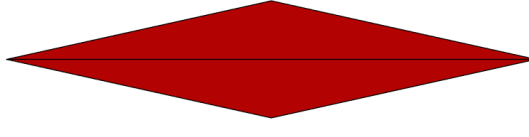
than its topology only. For all triangles whose quality improved, we add them to a set of new triangles, even if their quality is above the quality threshold. This set can then be processed in another pass in alg. 9.

Algorithm 2 Topological pass on triangular meshes

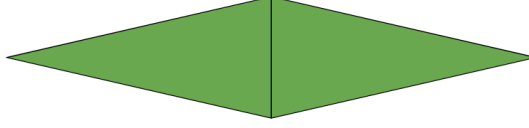
Require: A a set of triangles of the mesh

```

function TOPOLOGICALPASS2D( $A$ )
    changed  $\leftarrow$  false
     $E \leftarrow$  set of all edges of triangles in  $A$ 
     $A_{new} \leftarrow \{\}$ 
    for all  $e \in E$  do
        if  $e$  still exists then
            attempt to flip  $e$                                  $\triangleright t_1, t_2$  created by flipping edge  $e$ 
             $A_{new} \leftarrow A_{new} \cup t_1, t_2$ 
            changed  $\leftarrow$  true
            if  $Quality(t_1, t_2)$  did not improve then       $\triangleright$  Ensure mesh improvement in world space
                revert operation
            end if
        end if
    end for
    return the surviving elements of  $A \cup A_{new}$  and changed
end function
```



(a) 2 triangles of bad quality



(b) 2 better triangles after edge flip

Figure 4.2: Improving topology by edge flip

4.3.2 Insertion pass

For the two-dimensional insertion pass, presented in alg. 3, the idea is similar to its original three-dimensional implementation. We first attempt to dig a cavity, which is in turn filled with new elements of better quality. The key part of this algorithm is cavity digging, as filling it up simply consists of connecting the new point p located at the centroid of the triangles of A to the edges of the previously dug cavity. To find which elements belong to a cavity, the *FindFaceWithP* function is inspired by the *Bowyer-Watson* algorithm [2]. We start from the first element of the cavity, t , and mark it as visited. Then, we iterate through its neighbors and check whether, one they never have been visited, and two their circumcircle contains the new point p . If this is the case, we add this neighbor to the cavity and recursively treat its own neighbors as candidates for the cavity. The search ends when no new circumcircle contains p . This process

is illustrated in fig. 4.3a. Once completed, the result of the smoothed-out vertex p added to the mesh can be seen in fig. 4.3b.

Algorithm 3 Insertion pass on triangular meshes

Require: A , a set of triangles of the mesh

```

function INSERTIONPASS2D( $A$ )
     $A_{new} \leftarrow \{\}$ 
    for all  $t \in A$  do
         $p \leftarrow$  centroid of  $t$ 
         $D \leftarrow FindFaceWithP(D, t, p)$ 
        for all  $f \in D$  do
             $delete f$                                  $\triangleright$  creates a cavity
        end for
        for all  $e \in$  cavity's edges do
            add face  $f'$  with  $p, e$ 
             $A_{new} \leftarrow A_{new} \cup f'$ 
        end for
         $Smooth(p)$ 
    end for
    return the surviving elements of  $A \cup A_{new}$ 
end function

function FINDFACEWITHP( $D, f, p$ )
    if visited( $f$ ) or !contains( $p$ ) then
        return
    end if
    visited( $f$ )  $\leftarrow True$ 
     $D \leftarrow f$                                  $\triangleright$  we add  $f$  to the cavity
    for all  $adj \in$  adjacent faces do
         $FindFaceWithP(D, adj, p)$ 
    end for
end function
```

4.3.3 Smoothing pass

The last pass to discuss is the *smoothing pass*. In this part of the program, we attempt to regularize the point distribution through the mesh. For the triangular mesh implementation, we kept it simple and made it so that any point p to be smoothed is moved to the average position of its neighbors.

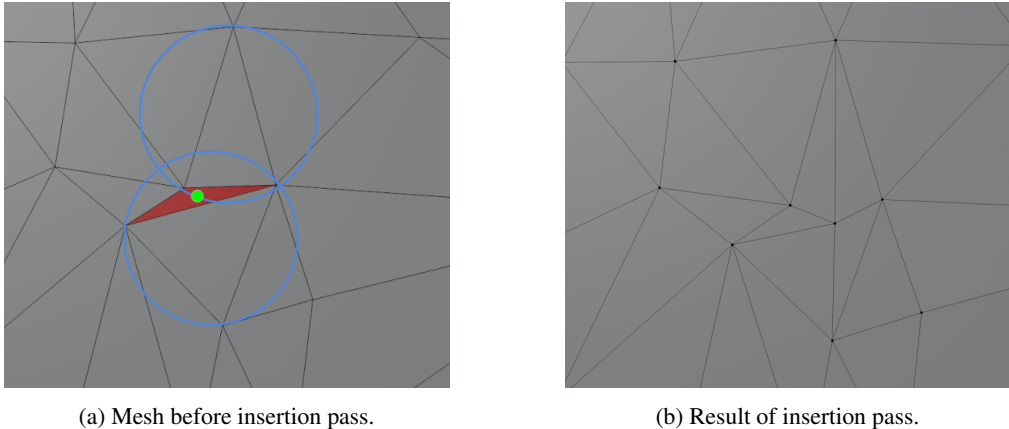


Figure 4.3: 2D Cavity building with successive circumcircles for the insertion pass. In green the new vertex added to the mesh to remove the bad triangle in red. After removal, the new point is connected to the cavity and smoothed.



Figure 4.4: Vertex smoothing on 2D meshes

4.4 Tetrahedral meshes

This section describes the implementation of the topological, insertion and smoothing passes with tetrahedral meshes. For clarity, all the material space checks presented in section 4.2 are omitted. In reality, for each mesh operation presented below, a validity check on the control mesh is performed to ensure bijection.

4.4.1 Topological pass

In the topological pass, the aim is to perform flips such that we can transform edges into faces or vice versa. These operations, illustrated in fig. 4.5, can be described as follow:

- **2-3 flip:** Transforms a face between 2 tetrahedra into an edge between 3 tetrahedra.
- **3-2 flip:** Reverse operation to the 2-3 flip, transforms an edge between 3 tetrahedra into a face between 2 tetrahedra.
- **Multi-face removal:** Generalization of the 2-3 flip, transforms n faces into an edge incident to $n + 2$ tetrahedra.

- **Edge removal:** Generalization of the 3-2 flip and reverse operation to the multi-face removal, transforms an edge incident to n tetrahedra into $n - 2$ faces between $2n - 4$ tetrahedra.
- 2-2 and 4-4 flips: Switches the direction of a group of tetrahedra, this operation is used in [12] but not in this implementation as they were used as boundary operations and our handling of surface elements differed from the original implementation.

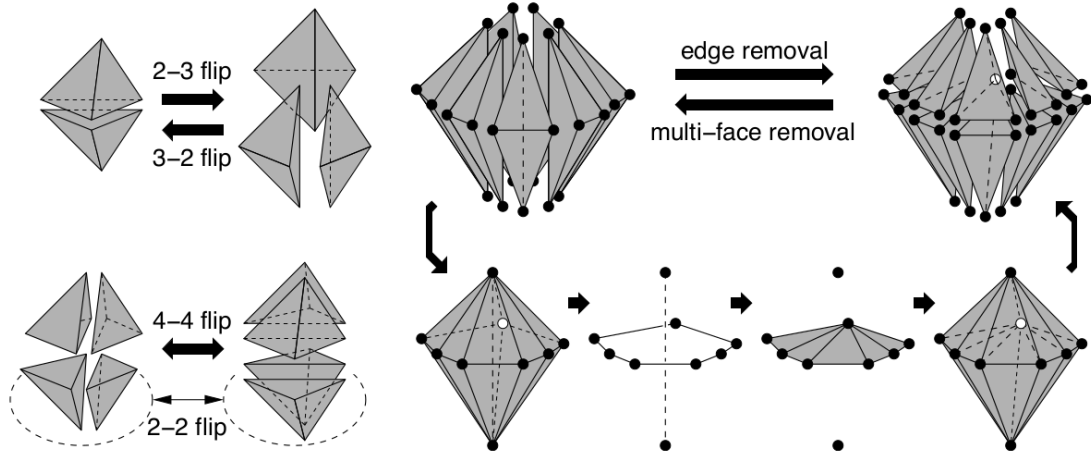


Figure 4.5: Mesh operations used, taken from [12]

A pass, described in alg. 4, tries to remove each edge and face of a tetrahedron. To remove an edge e , it goes through the steps of alg. 5. We first compute the *one ring* around e . It is composed of the vertices adjacent to e without being connected to the edge. Shewchuk [10] mentions that a ring size greater than 7 vertices rarely improves the mesh quality and is not worth the processing cost. After splitting e , we must find the collapse direction resulting in the smallest local energy. To do so, we collapse the newly added vertex in the direction of all the vertices composing the one ring around it and compare the results, storing the best halfedge to collapse. In the end, we ensure that the energy of the mesh around e has improved. If that is not the case, the operation is rolled back. As for the face removal, we compare the resulting energy between a simple 2-3 flip and the multi-face removal. If neither operation improves the mesh energy, none is chosen. The multi-face removal, described in more detail in [10], consists of finding the faces that are *sandwiched* between two vertices a and b . From [10], "[...] a triangular face f is *sandwiched* between a and b if the two tetrahedra that include f are $\text{conv}(f \cup a)$ and $\text{conv}(f \cup b)$ ". With the operator $\text{conv}(f \cup v)$ giving the tetrahedron composed of the vertices of the triangular face f and a vertex v of the mesh. Once we have found all the sandwiched faces, they are removed via a combination of 2-3 and 3-2 flips.

Algorithm 4 Topological pass on tetrahedral meshes

Require: A , a set of tets of the mesh

```

function TOPOLOGICALPASS( $A$ )
     $A_{new} \leftarrow \{\}$ 
    for all  $t \in A$  do
         $E \leftarrow$  edges of  $t$ 
         $F \leftarrow$  faces of  $t$ 
        for all  $e \in E$  do
            if  $e$  exists then
                 $changed \leftarrow RemoveEdge(A_{new}, e)$ 
            end if
        end for
        if  $changed$  then
            continue
        end if
        for all  $f \in F$  do
            if  $f$  exists then
                 $changed \leftarrow RemoveFace(A_{new}, f)$ 
            end if
        end for
    end for
    return the surviving elements of  $A \cup A_{new}$ 
end function

```

Algorithm 5 Edge removal on tetrahedral meshes

Require: $added$, a set of tets, e , the edge to remove

```

function REMOVEEDGE( $added$ )
     $m \leftarrow OneRing(e)$ 
     $q_{old} \leftarrow Quality(mesh)$ 
    if  $m > 7$  then
        return                                 $\triangleright$  From [10], after  $m > 7$  the mesh rarely improves
    end if
     $v \leftarrow SplitEdge(e)$ 
     $h \leftarrow FindCollapseDirection(v)$            $\triangleright$  Find the halfedge to collapse giving the best quality
     $Smooth(v)$ 
    if  $Quality(mesh) < q_{old}$  then
        rollback operation
        return False
    end if
     $added \leftarrow$  tets around  $v$ 
    return True
end function

```

4.4.2 Insertion pass

As described above, the insertion pass consists of digging a cavity and filling it up anew with elements of lower energy. This allows us to break from local optima that could be reached in the other passes by

adding new tetrahedra. With it, we create a more drastic change in topology which opens up a new set of remeshing opportunities that could not have been reached with the previous remeshing operations. To dig the cavity, we adapt the concept of *galaxies* presented by Hinderink and Campen[7]. The reasoning behind this choice was the complex original implementation from [12] who used a graph-based representation of the mesh to identify cavity elements. With the data structure used in this project, following the same approach would have been overtly complex and would not use the more recent and easier approaches at our disposal. Starting from a list of tetrahedra of high energy, we construct a set of *stars*, an aggregation of mesh elements, united in a common *galaxy*. To build them, we use their *chebyshev center*.

4.4.2.1 Chebyshev Center

The *chebyshev center* [4] of a star is the center of its largest inscribed sphere. In fig. 4.6, we can see its use to determine whether a cavity is star-shaped. Star-shapedness consists in the capacity for a cavity to be filled with tetrahedra without them overlapping each other or the existing mesh around the cavity. To find the chebyshev center, we take the boundary of the cavity and compute its inscribed sphere. A strictly positive value for r means the cavity is star-shaped. However we set a threshold for the radius to avoid filling the cavity with too small tetrahedra, at risk of being degenerate or of high energy.

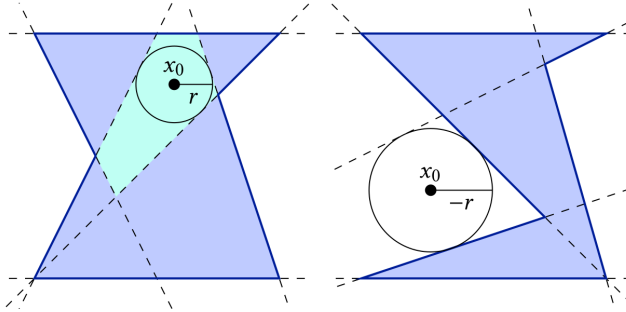


Figure 4.6: Star-shapedness tested with the chebyshev center, taken from [7]. A cavity is star-shaped if it holds an inscribed sphere of radius $r > 0$ with chebyshev center x_0 .

4.4.2.2 Insertion algorithm

The insertion algorithm is composed of three substeps: the cavity digging, the cavity filling, and a topological pass. For the first step (alg. 6), from each tetrahedron in A we start growing a star. This means that at first, each star has a size of one. To add to it, we want to add the neighboring tetrahedron that is the most likely to maintain star-shapedness. [7] use the following equation (eq. 4.1): Among the faces of the tetrahedra from a star S , we search the face whose incident tetrahedron is the least likely to break the star conditions, with n_f the normal of a triangle f , a_f a point on its image and x_0 the chebyshev center. The candidates f^* are presented as a sorted list, where we drop any element already contained in a star. If the end of the list is reached, then no additional element is joined to the star and the procedure ends.

$$f^* = \arg \max_f n_f^T x_0 - n_f^T a_f \quad (4.1)$$

Once the galaxy is fully computed, we remove all the tetrahedra contained in the stars, hollowing out the mesh.

Algorithm 6 Cavity digging on tetrahedral meshes

Require: A , a set of tets from the mesh

```

function CAVITYDIG( $A$ )
     $N \leftarrow 5$ 
     $G \leftarrow \{\}$                                  $\triangleright$  Empirically set, controls the size of the stars
    for all  $t \in A$  do                       $\triangleright$  create galaxy
        if  $t \notin S, \forall S \in G$  then
             $S' \leftarrow \{t\}$                        $\triangleright$  Create new star
            do
                 $t' \leftarrow FindNext(t)$ 
                 $S' \leftarrow S' \cup \{t'\}$ 
            while  $StarShaped(S')$  and  $S' < N$ 
             $G \leftarrow G \cup S'$ 
        end if
    end for
    for all  $S \in G$  do                       $\triangleright$  dig cavity
        for all  $t \in S$  do
             $DeleteTet(t)$ 
        end for
    end for
end function
```

Once the cavities are hollowed, for each star of the galaxy we add a new vertex at its chebyshev center and connect the vertices at the boundary of the cavity to this new element. Once the cavity is filled up, we smooth the created center to set an acceptable starting point for the last step of the insertion pass: a topological pass on the tetrahedra used to fill the cavity. Finally, if this pass did not improve the mesh energy, the operation is rolled back to its previous state.

Algorithm 7 Cavity Filling on tetrahedral meshes

Require: G , a galaxy

```

function CAVITYFILL( $G$ )
    for all  $S \in G$  do
         $c \leftarrow$  chebyshev center of  $S$ 
         $A' \leftarrow \{\}$ 
        AddVertex( $c$ )
        for all  $b \in$  boundary faces of  $S$  do
             $t' \leftarrow$  AddTet( $c, b$ )
             $A' \leftarrow A' \cup \{t'\}$ 
        end for
        Smooth( $c$ )
         $i \leftarrow 2$ 
        do
             $changed \leftarrow$  TopologicalPass( $A'$ )
             $i \leftarrow i - 1$ 
        while  $i > 0$  and  $changed$ 
    end for
    if  $Quality(G) < q_{old}$  then ▷  $q_{old}$  is the quality of the galaxy before the pass
        Rollback operation
    end if
end function
```

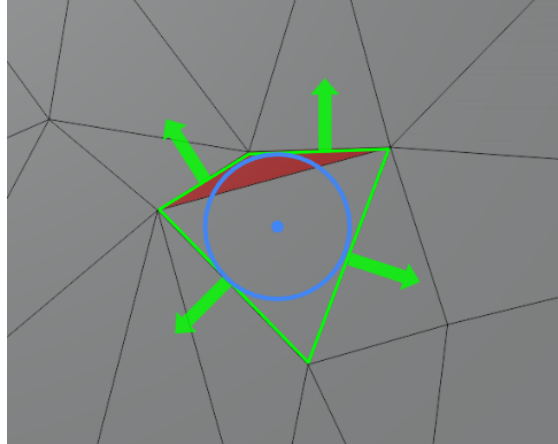


Figure 4.7: Boundary of a cavity (green) with its inscribed sphere (blue).

4.4.3 Smoothing pass

For the last pass of the algorithm, as presented in alg. 8, we go through all the remaining tetrahedra from A . In A are contained all the tetrahedra added or altered during the previous topological, contraction, and insertion passes. In this step, the goal is to smooth out the vertices of the list. To do so, we use the *chebyshev center* presented in sec. 4.4.2.1. We treat the neighboring tetrahedra to the vertex v we want to smooth as a cavity similar to the insertion pass (see fig. 4.8) and move v to the position of the chebyshev

center. This pass is the last to be applied to the list A as it expends it exponentially. For each vertex smoothed, we add its neighbors to A . Even after removing duplicates, this is by far the operation that changes the list the most and thus impacts performances.

Algorithm 8 Smoothing pass on tetrahedral meshes

Require: A , a set of tets of the mesh

```

function SMOOTHINGPASS( $A$ )
     $A' \leftarrow \{\}$ 
    for all  $t \in A$  do
         $V \leftarrow$  vertices of  $t$ 
        for all  $v \in V$  do
             $N \leftarrow$  neighboring tets of  $v$ 
             $q_{old} \leftarrow Quality(N)$ 
             $Smooth(v)$ 
            if  $Quality(v) < q_{old}$  then
                Rollback operation
                continue
            end if
             $A' \leftarrow A' \cup N$ 
        end for
    end for
    return the surviving elements of  $A \cup A'$ 
end function

```

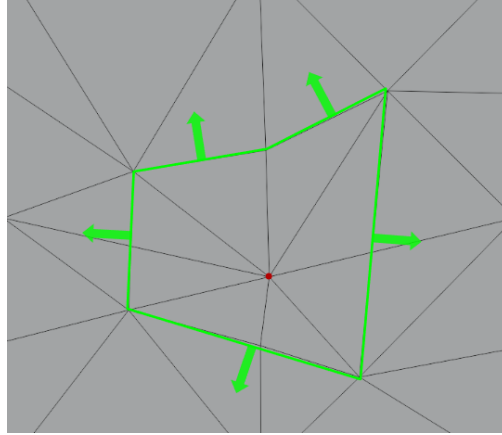


Figure 4.8: Boundary (green) used to find the chebyshev center during smoothing pass on a vertex (red).

4.5 Complete algorithm

Now that all of its parts are introduced, we can go through the complete flow of the remeshing algorithm (alg. 9). We iterate through the list A , sorted based on its elements' quality which will reduce and expand at each pass. A contains at first only the element of bad quality we want to get rid of but will vary in size after each mesh operation. Because as we alter the mesh, we also change the neighbors to the remeshed

element, and thus an improvement can be required on those too. Note: A may not only contain elements of quality below q_{min} , Wicke et al.[12] mention that their experiences showed some bad elements can only be improved by also altering their neighbors.

Algorithm 9 ImproveElement: Mesh improvement algorithm

Require: t an element of bad quality, N the number of remeshing iterations

```

function IMPROVEELEMENT( $t$ )
     $A \leftarrow \{t\}$ 
    for  $i \leftarrow 0$  to  $N$  do
        do
             $A \leftarrow TopologicalPass(A)$ 
            if  $Quality(A) \geq q_{min}$  then ▷  $Quality(A)$  returns the worst element of A
                return
            end if
        while  $TopologicalPass(A)$  changes the mesh
         $A \leftarrow ContractionPass(A)$ 
        if  $Quality(A) \geq q_{min}$  then
            return
        end if
         $A \leftarrow InsertionPass(A)$ 
        if  $Quality(A) \geq q_{min}$  then
            return
        end if
         $A \leftarrow SmoothingPass(A)$ 
        if  $Quality(A) \geq q_{min}$  then
            return
        end if
    end for
end function

function CONTRACTIONPASS( $A$ )
     $E \leftarrow$  set of all edges of elements in  $A$ 
    for all  $e \in E$  do
        if  $e$  still exists then
            attempt to contract  $e$ , smooth resulting vertex
        end if
    end for
    return the surviving elements of  $A$  and the mesh elements modified by edge contraction
end function

```

To improve an element t of the mesh, alg. 9 uses an iterative process where a list of elements goes through a succession of passes to locally improve quality. Note that [12] uses a value of $N = 10$ but it was adapted in this implementation due to performance. In the *Contraction pass*, the idea is to try to contract each element's edges to attempt to get rid of those that are close to being degenerated. This pass was not presented in its own section unlike the others as its implementation is similar regardless of the dimensionality of the mesh.

5

Results

This chapter presents the experiments run with the algorithm, on two- and three-dimensional meshes, as well as discusses the results obtained.

5.1 Triangular meshes

In this section, I'll describe the two experiments made in 2D and show the search for the optimal value of minimal quality. Mentioning that 2D was the stepping stone into the project and not many experiments were run. The implementation of the algorithm for triangle meshes served as a stepping stone into the more complex field of tetrahedral meshes. As such, not much experimentation was run with this implementation since it served more as a proof of concept. Two experiments were led with the two-dimensional remeshing algorithm: stretching the mesh and compressing it. In both cases, the goal was to empirically determine an acceptable value for the remeshing threshold q_{min} . Each experiment is run through iterative timesteps, defining the harshness of each deformation step and only the boundary vertices are moved by the deformation, handling the positions of the rest of them is left to the remeshing. At each time step, first, the deformation is applied to the mesh, and after this comes a remeshing pass. This composition can be seen in figure 5.1.

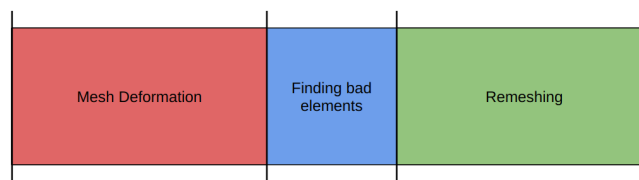


Figure 5.1: Timestep composition

5.1.1 Stretch

In this first experiment, the rectangular base mesh (fig. 5.2a) is stretched horizontally by a factor of 1.5. All of the stretching comes by moving the right boundary of the mesh. A real-life representation could be thought of as the left boundary being anchored and the right being pulled. To approximate physical properties, the boundaries perpendicular to the stretching direction are bent into a concave parabola as it would in an elastic deformation. We indeed see in figure 5.2b that most of the low-quality elements and thus remeshing performed are situated near the deformed parts of the mesh: the top, bottom, and right boundaries. We can also note some flips as well as additional geometry, meaning that both the topological and insertion pass influenced the remeshing.

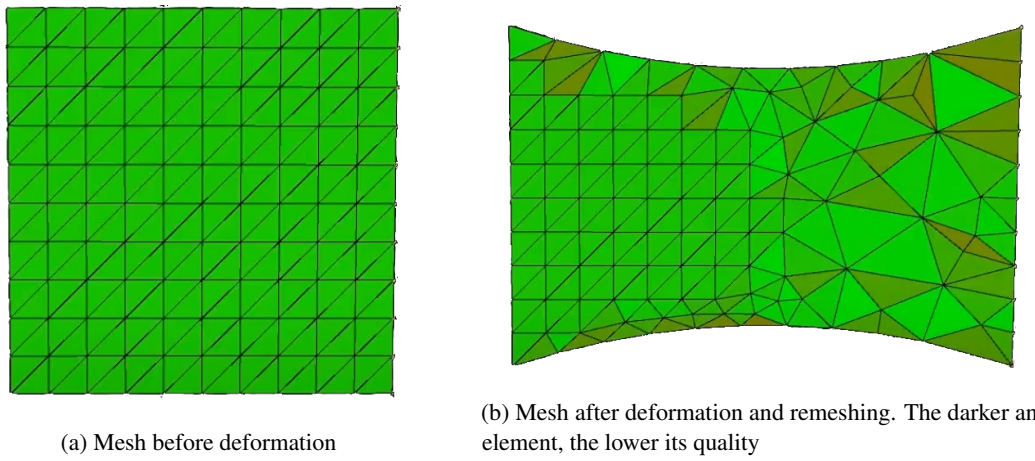


Figure 5.2: 2D stretch experiment

5.1.2 Compress

In this experiment, opposite to the stretching done before, we compress the mesh by moving the rightmost boundary to 66% of the initial mesh length. Similar to before, the left boundary stays immobile whereas the top and bottom boundary are bent to a parabola. For this situation, to simulate the material being pushed out by the compression, the parabola takes a convex shape. Similar to the stretch experiment, most of the work is done near the boundaries. We also have a clear show of the work of the contraction pass. When counting the number of triangles for a horizontal line going through the middle of the mesh, the number decreases from 20 to 14. This means that the triangles compressed by the moving edge have been removed by contracting one of their edges during the contraction pass. We can also note that the result of the remeshing differs significantly between the top and bottom boundaries. This highlights a point, which will also appear later for the tetrahedral meshes, of the remeshing results depending on initial conditions and some operations unlocking new possibilities at later timesteps that could be missed without them.

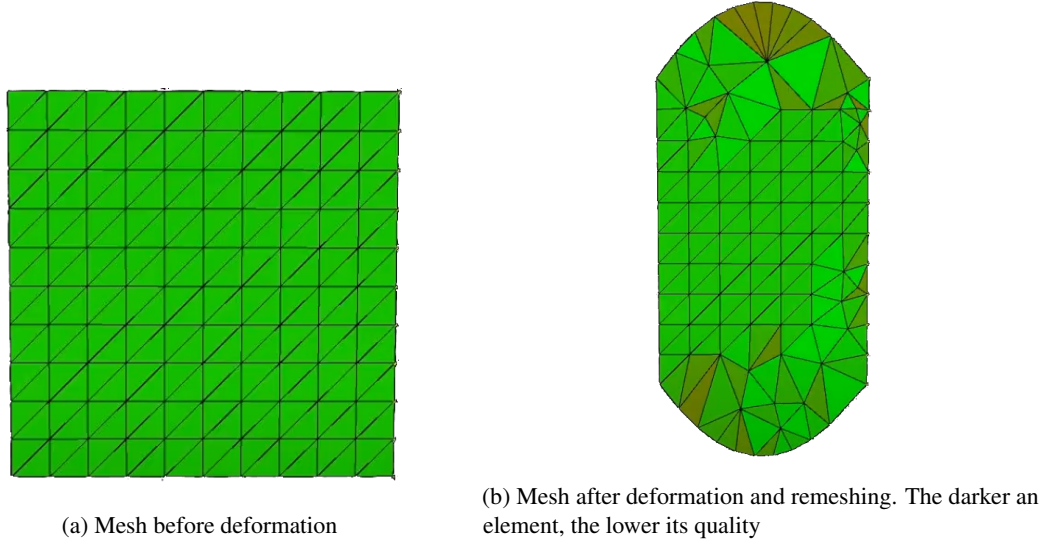


Figure 5.3: 2D compress experiment

5.1.3 Finding the right threshold

This last experiment on triangle meshes was run with the compress setting described above. The goal for it is to find the best value for q_{min} , the threshold responsible for adding elements to the list of elements to be processed in the remeshing pass. We need to fine-tune between a value too low, not allowing enough remeshing thus not improving mesh quality, and a value too high not realistically achievable triggering useless remeshing operations without actually improving topology. As presented in section 3.2, the quality of a triangle ranges between 0 and 1. The compressing experiment was run with a value of q_{min} from 0.1 to 0.7 with the same number of timesteps in each run. Higher values were not deemed interesting as they exceeded or were close to the initial mesh quality of ~ 0.85 , thus not being realistically reachable. Observing the results presented in figure 5.4, we can split them into three categories:

- **Close to degeneracy:** With q_{min} equal to 0.1 or 0.2 (first row of fig. 5.4), the threshold is so low that it accepts almost degenerate element into the mesh. This can lead to the situation where performing a remeshing worsens the situation as it induces inverted elements faster than the mesh deformation.
- **Optimal threshold:** For values ranging between 0.3 and 0.55 (middle rows of fig. 5.4) we see that the remeshing is still capable of maintaining the desired mesh quality even with the deformation at its maximum. Note that with $q_{min} = 0.4$, the threshold is not reached at later stages but still can be reached for higher values. An explanation can be found in the hill climbing principle. A remeshing operation could at a time t be seen as the best choice, only to be at a later time $t + n$ restricting a more efficient operation. That is why 0.4 still can be included in this category as the threshold is neither too restrictive nor tolerant but only depends on initial mesh configuration.
- **Unreachable threshold:** Values ranging from 0.6 and above (last row of fig. 5.4), although the desire behind them is to maintain high mesh quality, show that there exists a point where this desire is simply too much and cannot be fulfilled. They, while performing more operations than the other categories, produce worse results than lower thresholds situated in the optimal category. This is due to the program trying its best to reach an acceptable mesh quality, performing as many remeshing steps as possible and diverting from the regular initial mesh. This irregular mesh is more likely to create even worse irremovable elements after the next deformation step.

From the optimal threshold category, we can determine that a value for q_{min} near 0.5 is the best choice. We want the best possible quality with the best performances. With $q_{min} = 0.55$, we get closer to the upper limit and might risk losing the capability to reach it after deformation.

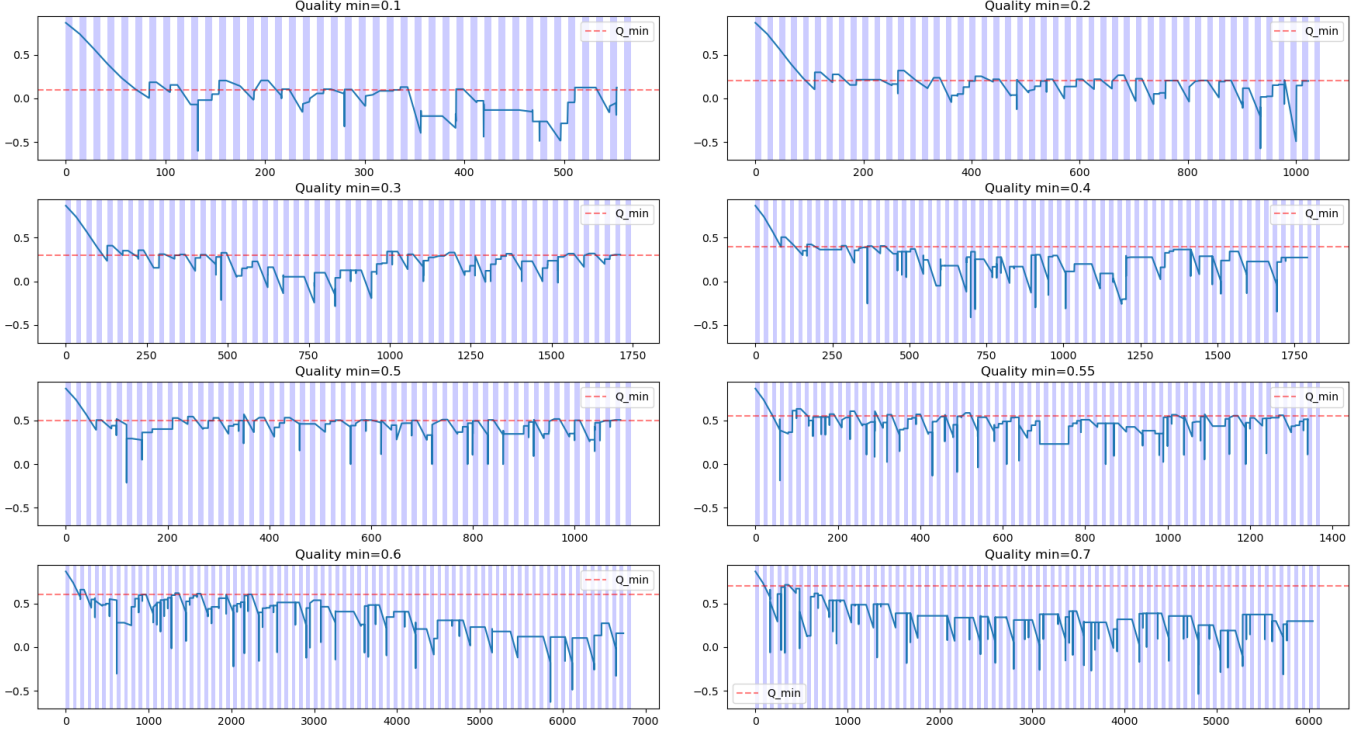


Figure 5.4: Evolution of the quality for different thresholds. The y -axis shows the quality of the worst mesh element, the x -axis shows the number of mesh operations performed. Two measures are taken per timestep: one after the deformation and one after remeshing. Deformation often creates near-degenerate or inverted elements, which can be in turn corrected by remeshing. We also note that increasing the threshold raises drastically the amount of remeshing operations performed and produces a worse quality than the more attainable ones.

5.2 Tetrahedral meshes

For 3D meshes, each deformation applied to the mesh is either a twist or a stretch. Our goal through these experiments is to find an optimal threshold for the energy, evaluating the impact of the timestep size and deformation intensity as well as the impact of the control mesh.

5.2.1 Performance of passes

Using a hill climbing method with iterative passes means that we have to reject a lot of potential remeshing operations. This is especially true for the *topological pass* where there are multiple operations to consider and to compare. Having a broad choice with only a single chosen option will inevitably result in computations that were done "for nothing" as they will not contribute to the remeshing process. Due to

the costs in performance, this implementation requires us to adapt the mesh to best suit our experiments without losing either time or quality. Details of these adaptations are presented in the section 5.2.2.

5.2.2 Twist

This mesh deformation consists of rotating vertices along the z -axis, giving a spiraling look to the base mesh (figs. 5.5a and 5.5b). Two variants of the deformation were applied. First, a basic one in which the whole mesh rotates along the axis. Second, one where only the surface vertices were displaced, thus triggering more remeshing operations as the difference between the surface and inside increases. The first option was used in most experiments as it is more realistic from a physical standpoint. If in a section nothing about the deformation is mentioned, assume all the vertices were free of movement. Since we observed that most of the remeshing was happening near the boundary, we add an additional global refinement pass on the boundary tetrahedra (fig. 5.5c). This allows for more fine-grain remeshing where it is needed, without the additional cost induced by refining the full mesh.

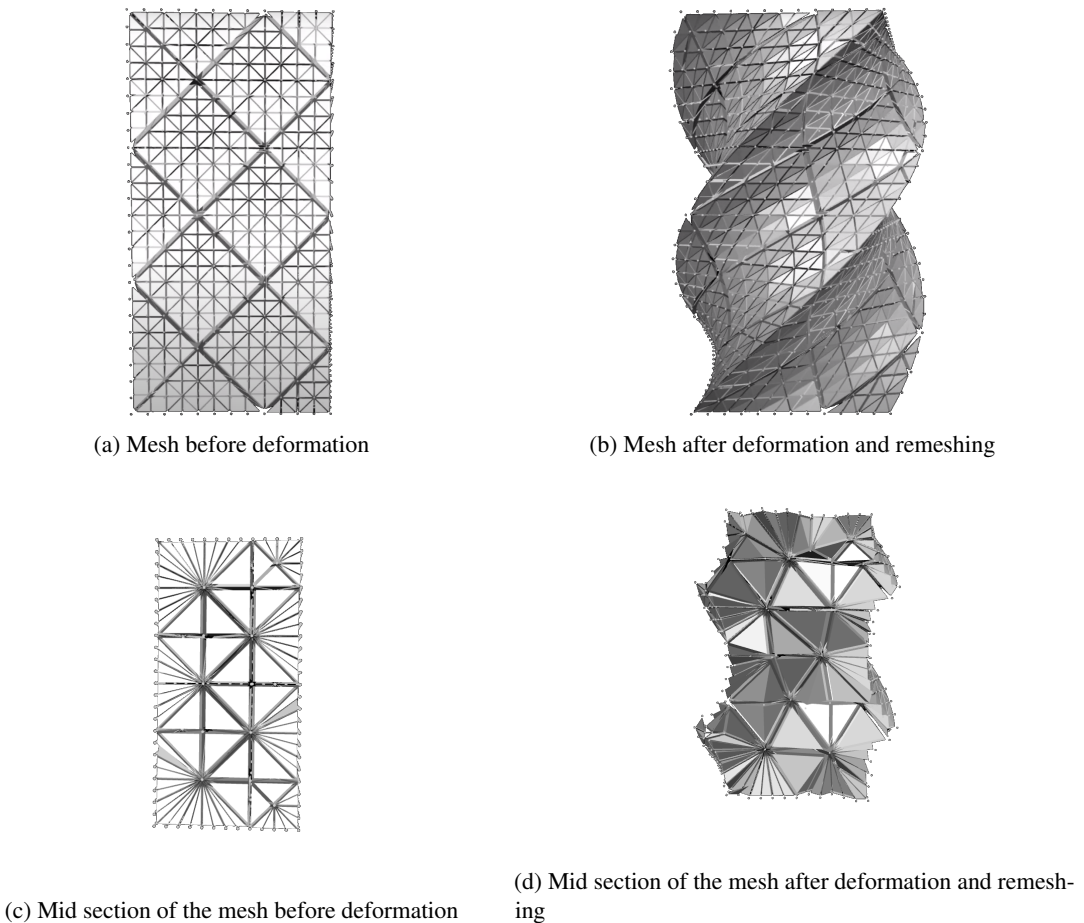


Figure 5.5: 3D twist experiment

5.2.2.1 Influence of the Energy Threshold

In this experiment, we aim to find the optimal value for the maximal energy threshold d_{max} . To do so, we applied the twist deformation to boundary vertices with increasing leniency towards difference to the reference regular tetrahedron. Moving only the surface vertices allows for more observations of the remeshing being performed and thus a better evaluation of the algorithm's adaptation. We rotated the boundary points 180° around the axis in 360 timesteps, giving a 0.5° increment per timestep.

In figure 5.6, we observe three categories of results:

1. **Unsuccessful remeshing:** With $d_{max} = 35$, the desired energy is too low and no remeshing step allows the mesh to go back to this state once the limit is crossed by many elements. In figure 5.6 top left, we see that the first crossing of the threshold can be recovered like any other value for d_{max} but as soon as multiple timesteps are unable to lower the energy it continuously increases in average.
2. **Partially successful remeshing:** With $d_{max} = 40$, we seem to be near the limit of energy the algorithm can recover from. In the first part, the deformation is salvageable but it reaches a state from which it is not able to come back, slipping into the first category of unsuccessful remeshing.
3. **Successful remeshing:** With $d_{max} \geq 45$, each crossing of the threshold is recovered from. With no sign of slipping into an endless loop of increasing energy.

These results show that a threshold of ~ 45 is the best choice in this situation. This value is in no way absolute as it must take into account the severity of the deformation. For more intense deformations, where greater energies are unavoidable, a d_{max} of 45 might give results of the first or second category.

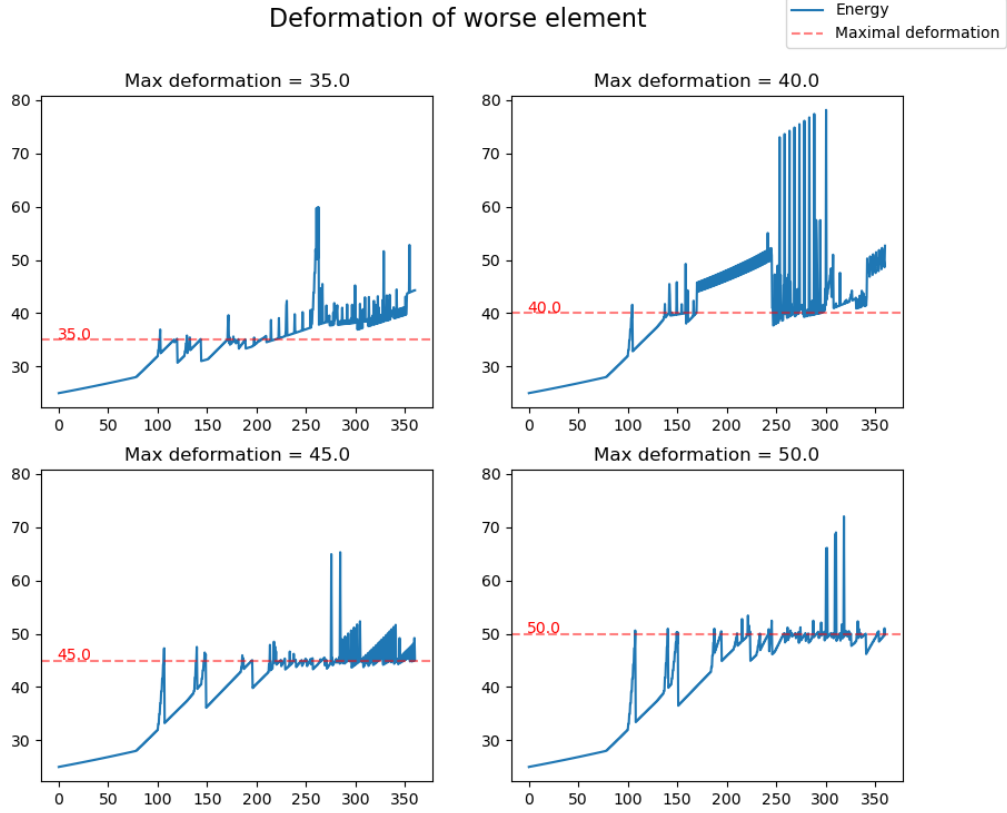


Figure 5.6: Comparison of energy for different threshold values during the spin. The x -axis represents the timestep progression, the y -axis shows the deformation energy of the worst element of the mesh. We observe that setting a value too low ($d_{max} = 40$) yields worse results than a higher and more adequate threshold ($d_{max} = 45$). Measures are taken before and after a remeshing step, resulting in the peaks and dips displayed by the energy.

5.2.2.2 Influence of the Timestep Size

In this second experiment, the goal is to evaluate the impact of the timestep size on performance and quality of the remeshing. To do so, the twist deformation is applied with different parameters shown in figure 5.7. For the half turns (rotation of 180°), the number of timesteps ranges from 9 to 1800 and is doubled for the full turn. This brings us to a rotation angle of 0.1° to 20° per timestep. For experiments with a low remeshing threshold or high deformation (figs. 5.7a and 5.7d), we get results of the unsuccessful remeshing category presented in the previous experiment where no matter the number of timesteps it is unable to recover from the high energy. We see that increasing the number of timesteps does not equate with better quality. This shows the limitation induced by local optima in hill-climbing methods. Based on the remeshing choices performed during previous iterations, some largely better options cannot be performed but are available to the ones who skipped some remeshing steps. In figure 5.7b is shown that the solution with d_{max} presented as a partially successful remeshing could be tipped into any other category based on the number of timesteps, fortifying its position as the limit between them. By increasing the

number of timesteps it now falls into the successful category whereas by decreasing it worsens its results. This highlights the trade-off between performance and quality as this shift in category comes at a great price in terms of execution time. Using the biggest number of timesteps possible can be used as a good approximation tool but is not to be treated as a golden rule. In the experiment with $d_{max} = 50$ (fig. 5.7c), it appears that the energy of the worst element, as well as the mesh, seems to plateau below the threshold with an exponential growth in time required. In this situation, using more timesteps is unnecessary as we could use the additional time freed by performing more passes of the algorithm, maybe giving an even better result. This plateau might be interpreted as the last acceptable energy for a tetrahedron. Any higher energy would trigger the remeshing after the next deformation step, thus bringing its quality below the threshold again.

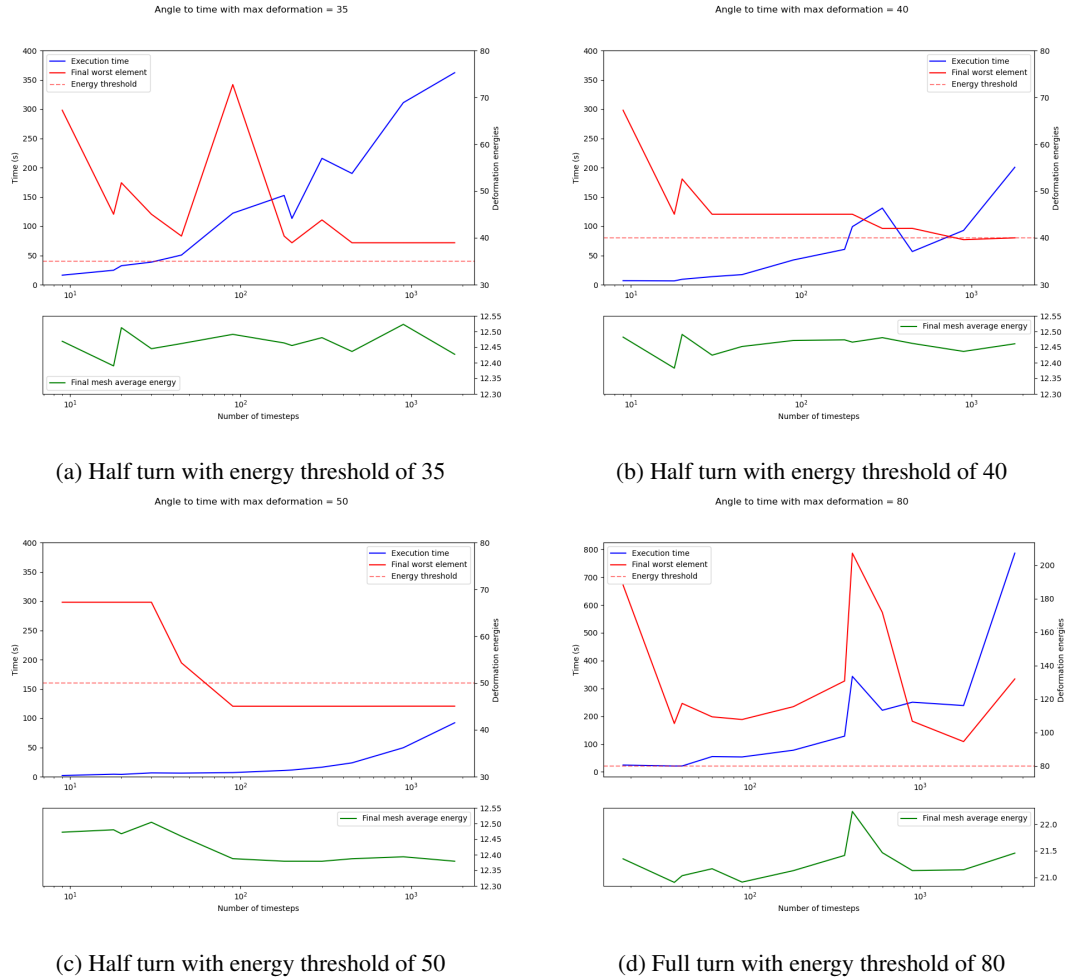


Figure 5.7: Comparison of execution time (blue), worst element energy (red) and average mesh energy (green) for varying timestep numbers. The x -axis shows the number of timesteps, the left y -axis the time in seconds, and the right y -axis the deformation energies

5.2.2.3 Handling greater deformations

For this last experiment with the twist deformation, we observe the impact of larger deformations on the remeshing algorithm. We took the lenient $d_{max} = 50$ from previous experiments and 0.5 increment timesteps. We see in figure 5.8 that larger deformations explode in terms of both energy and time, especially for the full turn. We notice here the limitations of this implementation as the only way to make bigger deformations work would be to set a high remeshing threshold that would result in visibly bad tetrahedra, rendering the remeshing almost useless given that the increase in mesh quality would not be worth the resources used.

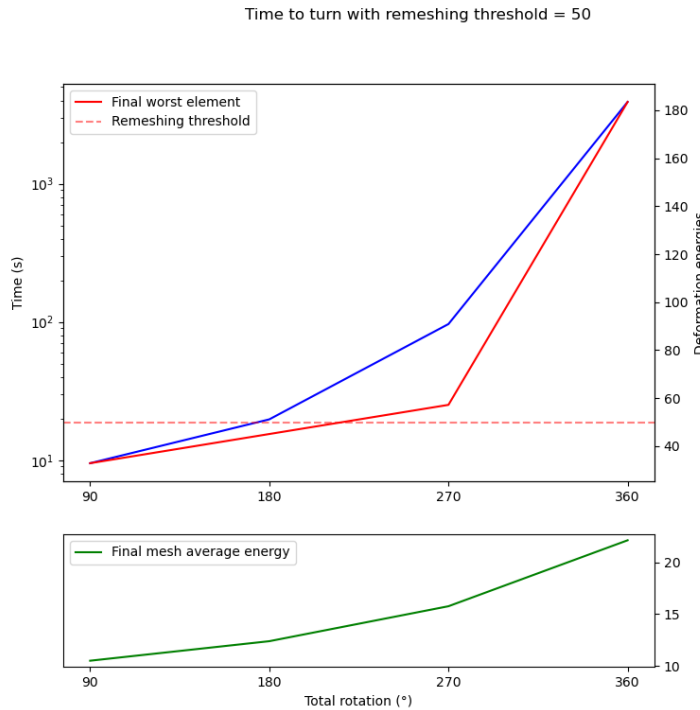


Figure 5.8: Evolution of performance of execution time (blue), worst element energy (red) and average mesh energy (green) with deformations ranging from 90° turns to 360°, in 90° increments.

5.2.3 Stretch

Similar to the two-dimensional implementation of section 5.1.1, for this mesh deformation the bottom boundary is pulled down while the sides are bent. This allows to emulate a plastic or elastic deformation of the object.

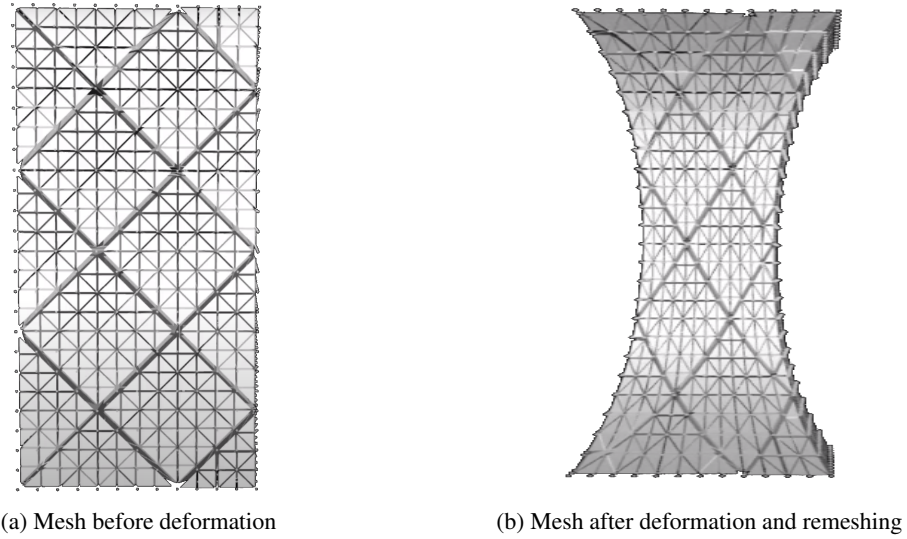


Figure 5.9: 3D twist experiment

5.2.3.1 Influence of the Energy Threshold

In this experiment, the mesh is stretched to 1.7 times its initial length with remeshing thresholds equal to 30, 35 and 40. All the runs were performed in 300 timesteps.

Similarly to the spin's results, we see again in the figure 5.10 the three categories set in the previous section (sec. 5.2.2.1): *unsuccessful*, *partially successful* and *successful remeshing*.

With a threshold value too low like $d_{max} = 35$, the remeshing is not able to keep control of the deformation, and the energy increases without showing signs of getting back to an acceptable level. When nearing the optimal value, the energy curve follows the threshold for a while before taking off.

With the results of this second experiment, we can generalize the behavior of the energy curve to identify whether an arbitrary value for d_{max} is optimal based on its curve. The procedure would be to start high and, as long as the curve stays in the 3rd category, lower it until we reach the 2nd category. If we ever overshoot and reach the 1st one, we then know to increase it again, following some kind of *binary search* methodology.

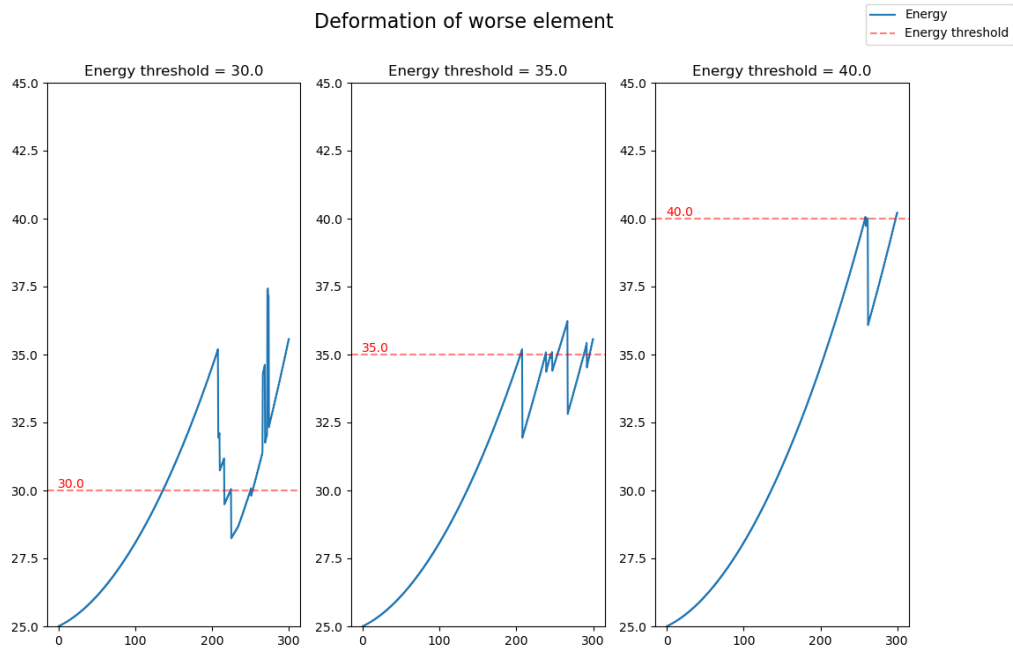


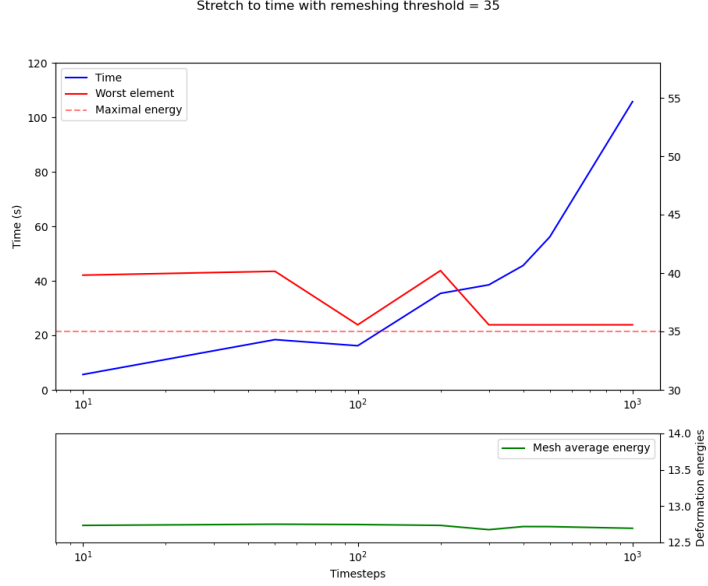
Figure 5.10: Comparison of energy for different threshold values during the stretch. The x -axis represents the timestep progression, the y -axis shows the deformation energy of the worst element of the mesh.

5.2.3.2 Influence of the Timestep Size

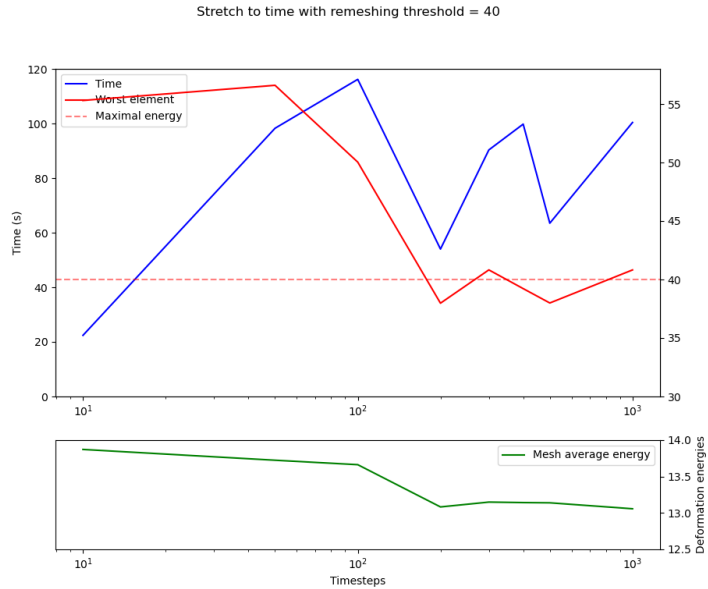
In this experiment, we tried stretching the mesh by a factor of 1.7 with varying numbers of timesteps, ranging from 10 to 1000. In figure 5.11, we see the results with two different thresholds. The first one (fig. 5.11a) takes a voluntarily low threshold to see if we can recover from the deformation with finer timesteps and on the second (fig. 5.11b) is the value we found to be on the limit of acceptability in the experiment of section 5.2.3.1.

In the first case, we observe that no matter the amount of timesteps, the algorithm is never able to reach an energy below the desired value of the energy. The highest numbers of timesteps are closer and the average mesh energy lower so we can assume that a high number of timesteps is the best choice in this situation but comes at an exponential cost in performance. If the curve's dynamics were to continue with bigger x values, then settling for the smallest time-to-energy ratio would be even more efficient. We can observe a bump in energy at 200 timesteps. This is another example of a hill-climbing algorithm deciding on a local optimum leading to worst solutions in the future. Adjusting the timestep size opens possibilities that smaller or bigger amounts would not offer, thus creating a bump at only $x = 200$. In the second case, this variety of available solutions is even clearer. Since we are at the limit of the threshold's remeshing trigger, solutions vary greatly from one another based on the timestep size. We see that lower values yield significantly worse results by crossing too harshly the limit set by the threshold and cannot be recovered from, triggering remeshing on bigger sets of tetrahedra and increasing time consumption. For higher values, we do not see a clear favorite in terms of energy or time. We do note that failing to reach the desired energy results in bigger time requirements. This is due to the implementation of the algorithm, once we reach an acceptable energy or treat all the tetrahedra of high energy the execution stops without going through the remaining passes. Failing to treat even one element would result in additional remeshing

passes impacting performance.



(a) Stretch of factor 1.7 with energy threshold of 35



(b) Stretch of factor 1.7 with energy threshold of 40

Figure 5.11: Comparison of time (blue), worst element energy (red) and average mesh energy (green) for varying timestep numbers. The x -axis shows the number of timesteps, the left y -axis the execution time in seconds, and the right y -axis the deformation energies

5.2.3.3 Handling bigger deformations

In this last experiment, we evaluate the remeshing's capacity to handle greater stretching. Starting from the default experiment with $d_{max} = 40$ and 300 timesteps with a stretching factor of 1.7, we apply stretching ranging from 1.5 to 2 while adapting the number of timesteps. Failing to do so would be unfair as bigger deformations would be performed in bigger increments, which we have seen to lower the quality of the remeshing. The full conversion can be seen in table 5.1.

Stretching factor	1.5	1.6	1.7	1.8	1.9	2
Timesteps	265	283	300	318	335	353

Table 5.1: Stretching factor to timestep relation

Like with the twist deformation (sec. 5.2.2.3) we see that bigger energies quickly go out of control of the remeshing algorithm, both in terms of quality and performance. An interesting observation is that, although on average higher, the energy of the worst element of the mesh is lower with a factor of 2 than 1.9. We observe the vulnerability of the algorithm to its preceding operations. In this case, a tetrahedron might have been altered to lower its energy at a timestep t but the following deformation step created an even worse element. The inverse interpretation is also possible, by applying a big enough deformation, a problematic tetrahedron and its neighbors that could not be removed reached a state where the remeshing operation is possible and improves the mesh quality.

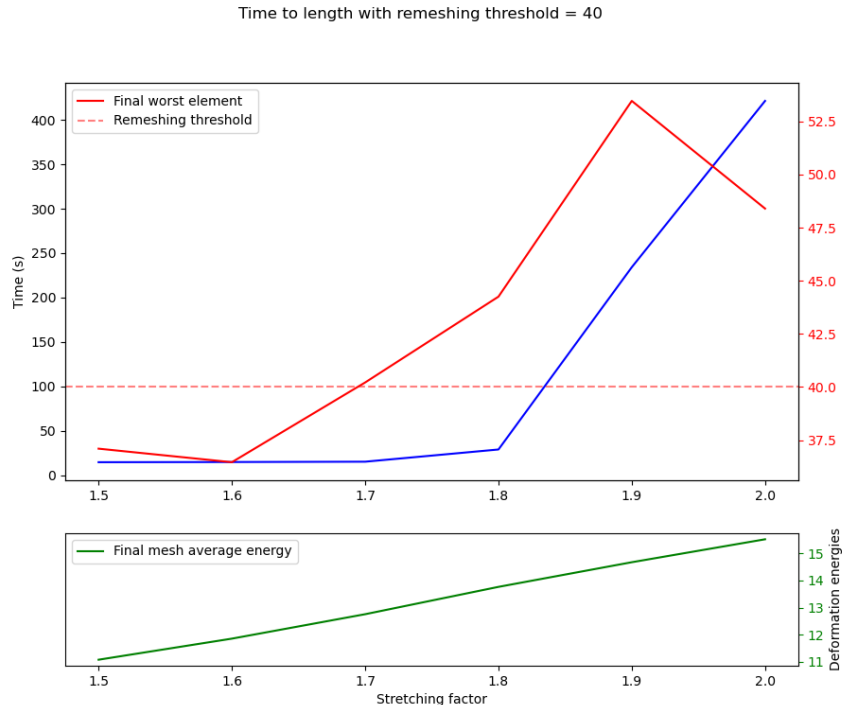


Figure 5.12: Evolution of performance of execution time (blue), worst element energy (red) and average mesh energy (green) with stretching factors ranging from 1.5 to 2, in 0.1 increments

5.2.4 Impact of the control mesh

Bijection of operation is ensured through the existence of both the material and world spaces. Validating each operation on the material space induces a performance overhead but also limits the range of operations available to the remeshing algorithm. If the best choice is refused in material space does the quality of the remeshing suffer from it or is it able to find alternatives to reach the desired energy?

We see in figure 5.13 that for a twist experiment, the version with the material space (in orange) can reach the same level of energy as the one without it (in blue). Not having this restriction allows for a quicker recovery but eventually this restriction yields similar results while only using revertible operations. This means that keeping a stack of the performed remeshing steps and going through it in reverse order would give us the initial mesh without changes in topology.

We observe here that the only additional cost of using the two spaces is resource-related. Specifically, it affects memory consumption, as a representation of the mesh is needed in both spaces, and performance, since each operation must be validated before being applied to the mesh.

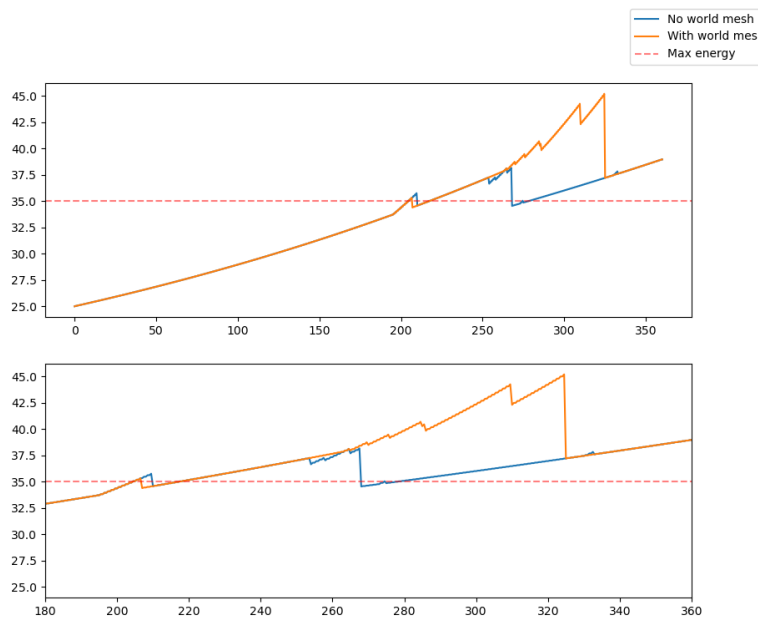


Figure 5.13: Evolution of the quality with and without using material space, for the full experiment (top) and a close view after the trigger of the remeshing (bottom). In orange the algorithm with a control mesh and in blue the algorithm without control mesh

5.2.5 Reverse deformation

The last experiment consists of taking the mesh obtained at the end of the twist deformation and reverse it to its initial cuboid shape, performing the inverse deformation to the twist experiment. We observed that the object returns to its initial shape but does not recover its initial topology. This can be explained by the difference between the average mesh energy in the cuboid mesh and the remeshing threshold. Since the first is lower than the threshold, there is no incentive for the remeshing to try to retrieve this state and will in place aim for a mesh energy situated right below the remeshing threshold.

6

Conclusion

In this work we presented an implementation of a local remeshing algorithm for injective deformations of both two- and three-dimensional meshes. Injectivity is ensured thanks to the representation of the 3D object in two different spaces, material and world spaces. The first one is responsible for validating remeshing operations applied to the second. The algorithm is a hill-climbing method in which bad elements of the mesh go through four successive passes, each one responsible for tackling a different approach to improve the mesh. The implementation was evaluated by subjecting the mesh to multiple deformations. Their goal was to identify optimal parameter values as well as evaluate the quality and performance of the remeshing.

6.1 Weaknesses and future work

Through our experiments, we observed situations in which the algorithm's implementation was not optimal, mainly two points: Performance and local optima. We saw that great deformations could not be recovered from, even with small timesteps, and that the algorithm was sensible to its configuration. Reducing the timestep size would not always yield results with improved quality. In some cases, finer deformation steps could actually perform worse than larger ones.

Performance is linked to the concept of hill climbing. Only taking steps in the summit direction means that any other step evaluated was run for nothing. If a hundred possible steps are available but only the last one leads us in the right direction, the 99 others were computed for nothing. And this right step at the time might not even be the best choice if we take into account the step after. In our implementation, a remeshing step at timestep t is not aware of the upcoming deformation step. This means that the next step might result in a worse mesh after remeshing than had we done nothing. This problem links both weaknesses of the project: by going in the wrong direction of local optima, we then have to perform more remeshing steps to recover thus, impacting performances.

A way of fixing this would be to have some kind of temporal knowledge. With it, we would be able to take into account preceding timesteps and approximate the next deformation step to better evaluate our remeshing choices. However, this does not improve the handling of big deformations. Improving performance would be beneficial for solving both the issue of treating big deformations as well as making wrong remeshing choices. By performing more remeshing passes we would be able to extend the treated area around the bad element and thus regularize it to avoid surprises at the next remeshing step. To take

again the hiker image, if more hikers are searching for the top of the hill, the chances of finding the summit increase.

6.2 Use of AI tools

Please note that the LLM ChatGPT was punctually used in the redaction of this report to improve the quality and readability of the text.

Bibliography

- [1] *Reviving the Search for Optimal Tetrahedralizations*. Zenodo, February 2020.
- [2] Calin Arens. The bowyer-watson algorithm; an efficient implementation in a database environment. 2002.
- [3] Adam W. Bargteil, Chris Wojtan, Jessica K. Hodgins, and Greg Turk. A finite element method for animating large viscoplastic flow. In *ACM SIGGRAPH 2007 Papers*, SIGGRAPH '07, page 16–es, New York, NY, USA, 2007. Association for Computing Machinery.
- [4] Stephen Boyd and Lieven Vandenberghe. *Convex Optimization*. Cambridge University Press, 2004.
- [5] Lori Freitag, Mark Jones, and Paul Plassmann. A parallel algorithm for mesh smoothing. *SIAM Journal on Scientific Computing*, 20(6):2023–2040, 1999.
- [6] Vladimir Garanzha, Igor Kaporin, Liudmila Kudryavtseva, François Protais, Nicolas Ray, and Dmitry Sokolov. Foldover-free maps in 50 lines of code, 2021.
- [7] Steffen Hinderink and Marcel Campen. Galaxy maps: Localized foliations for bijective volumetric mapping. *ACM Trans. Graph.*, 42(4), jul 2023.
- [8] Bryan Matthew Klingner and Jonathan Richard Shewchuk. Aggressive tetrahedral mesh improvement. In Michael L. Brewer and David Marcum, editors, *Proceedings of the 16th International Meshing Roundtable*, pages 3–23, Berlin, Heidelberg, 2008. Springer Berlin Heidelberg.
- [9] A. Rassineux. 3d mesh adaptation. optimization of tetrahedral meshes by advancing front technique. *Computer Methods in Applied Mechanics and Engineering*, 141(3):335–354, 1997.
- [10] Jonathan Shewchuk. Two discrete optimization algorithms for the topological improvement of tetrahedral meshes. 01 2002.
- [11] Justin Solomon, Leonidas Guibas, and Adrian Butscher. Dirichlet energy for analysis and synthesis of soft maps. *Computer Graphics Forum*, 32(5):197–206, 2013.
- [12] Martin Wicke, Daniel Ritchie, Bryan M. Klingner, Sebastian Burke, Jonathan R. Shewchuk, and James F. O'Brien. Dynamic local remeshing for elastoplastic simulation. *ACM Trans. Graph.*, 29(4), jul 2010.
- [13] Chris Wojtan and Greg Turk. Fast viscoelastic behavior with thin features. *ACM Trans. Graph.*, 27(3):1–8, aug 2008.